Chapter 2

Coupled Multilayer Resonators

Filters are very essential elements in many fields of RF/microwave engineering. The filters are used to separate/combine or select/reject signals at different frequencies in RF/microwave communication systems. Although the physical realization of filters at RF/microwave frequencies may vary, the circuit topology is common to all. This chapter is divided into several main topics about basic concept of coupled resonator. This part is compulsory to ensure that the objectives and the scope of this research are achieved.

2.1 Microstrip Lines

Microstrip lines become one of the most popular types of planar transmission lines primarily due to its ease to be fabricated, miniaturized and integrated with both passive and active microwave devices. The general structure of a microstrip line is illustrated in Figure 2-1. The bottom of the substrate is a ground plane and a conducting strip with a width W and a thickness t is located on the top of a substrate that has a relative dielectric constant ε_r and a thickness h.

If the dielectric substrate is not present ($\varepsilon_r = 1$), we would have a two-wire line consisting of a flat strip conductor over a ground plane, embedded in a homogeneous medium (air). This would constitute a simple TEM transmission line with phase velocity $v_p = c$ and propagation constant $\beta = k_0$.

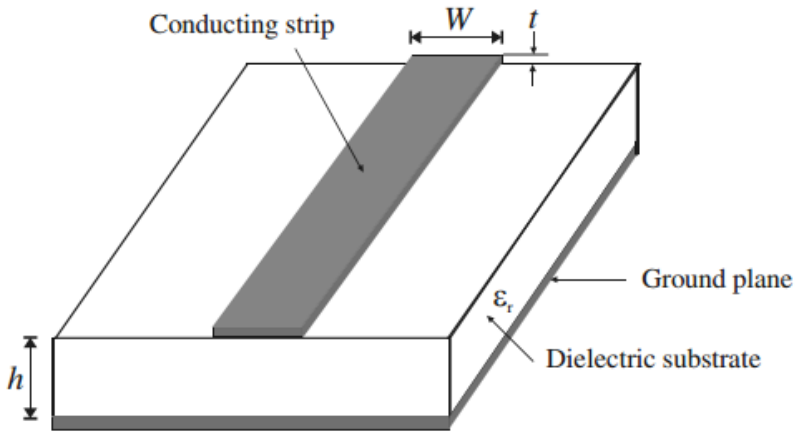

Figure 2.1 Microstrip line

This kind of elements present a number of characteristics among those we can mention: the ground plane below the current conductor traces prevents the excessive electromagnetic (EM) field leakage and thus reduces radiation loss. The severity of the leakage depends on the dielectric constants (ε_r) of the substrate. A higher dielectric constant substrate can minimize the EM field leakage and the coupling due to radiation.

2.2 Effective Dielectric Constant and Characteristic Impedance

Transmission characteristics of microstrips are described by two parameters, namely, the effective dielectric constant ε_{re} and characteristic impedance Zc, which may then be obtained by quasi-static analysis. In quasi-static analysis, the fundamental mode of wave propagation in a microstrip is assumed to be pure TEM. The above two parameters of microstrips are then determined from the values of two capacitances as follows

$$\varepsilon_{re} = \frac{C_d}{C_a} \qquad \text{.....(2-1)}$$

$$Z_c = \frac{1}{c\sqrt{C_a C_d}} \qquad \text{..... (2-2)}$$

in which C_d is the capacitance per unit length with the dielectric substrate present; C_a is the capacitance per unit length with the dielectric substrate replaced by air, and c is the velocity of electromagnetic waves in free space ($c=3.0 \times 10^8$ *m/s*).

This chapter describes coupled resonators to construct a BPF. The co-existence of electric and magnetic coupling scheme and the cross-coupling path are used to create the TZs for second-order design. A new approach was proposed to adjust the transmission-zero frequencies caused by the tapped-line feed. Controlling the length and the width of the resonator gap can effectively tune the transmission-zero frequencies in the stopband. Additionally, the resonators were also used to implement a second-order BPF design with a sharp transition for achieving superior passband selectivity.

2.3 Coupled Resonator Circuits

In general, figure 2-2 shows the coupling coefficient of coupled RF/microwave resonators,

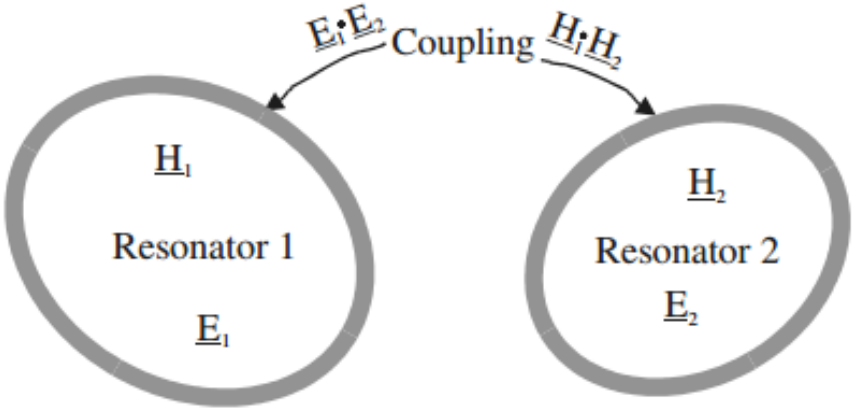

Figure 2.2 General coupled RF/microwave resonators where resonators 1 and 2 can be different in structure and have different resonant frequencies.

It may be much easier by using EM simulation or experiment to find some characteristic frequencies that are associated with the coupling of coupled resonators. The coupling coefficient can then be determined by adjusting the physical structure of the resonator when the relationship between the characteristic frequencies and the coupling coefficient is established.

2.3.1 Synchronously Tuned Coupled-Resonator Circuits

2.3.1.1 Electric Coupling

Figure 2-3(a) shows an equivalent lumped-element circuit model for electrically coupled resonators, where L and C are the self-inductance and self-capacitance respectively, so that $(LC)^{-1/2}$ equals the angular resonant frequency of uncoupled resonators, where C_m represents the mutual capacitance. If the coupled structure is a distributed element, the lumped-element equivalent circuit is valid on a narrow-band basis, namely, near its resonance. Now, if we look into reference planes T_1–T_1' and T_2–T_2', we can see a two-port network that can be shown by the following equations:

$$I_1 = j\omega C V_1 - j\omega C_m V_2 \quad \text{(2-3)}$$

$$I_2 = j\omega C V_2 - j\omega C_m V_1 \quad \text{(2-4)}$$

in which a sinusoidal waveform is assumed. (2-3) and (2-4) imply that the self-capacitance C is the capacitance seen in one resonant loop of Figure 2-3 when the capacitance in the adjacent loop is short-circuited. Thus, the second terms on the R.H.S. of (2-3) and (2-4) are the induced currents

resulting from the increasing voltage in resonant loop 2 and loop 1, respectively. From (8.32) four Y parameters can easily be found as

$$Y_{11} = Y_{22} = j\omega C \quad \text{.....(2-5)}$$

$$Y_{12} = Y_{21} = -j\omega C_m \text{.....(2-6)}$$

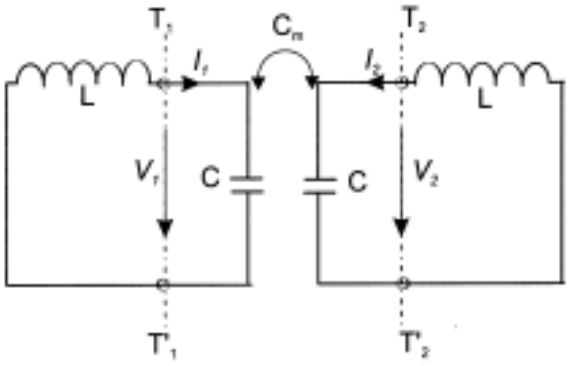

(a)

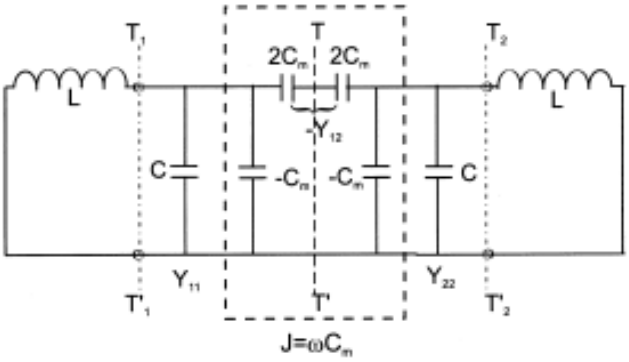

(b)

Figure 2.3 (a) Synchronously tuned coupled resonator circuit with electric coupling. (b) An alternative form of the equivalent circuit with an admittance inverter J= ωC_m to represent the coupling.

According to the network theory an alternative form of the equivalent circuit in Figure 2-3(a) can be obtained and is shown in Figure 2-3(b). This form yields the same two-port parameters as those of the circuit of Figure 2-3(a), but it is more convenient for our discussions. Actually, it can be shown that the electric coupling between the two resonant loops is represented by an

admittance inverter $J= \omega C_m$. If the symmetry plane *T–T'* in Figure 2-3(b) is replaced by an electric wall (or a short circuit), the resultant circuit has a resonant frequency

$$f_e = \frac{1}{2\pi\sqrt{L(C+C_m)}} \quad \text{.....(2-7)}$$

This resonant frequency is lower than that of an uncoupled single resonator. A physical explanation is that the coupling effect enhances the capability to store charge of the single resonator when the electric wall is inserted into the symmetrical plane of the coupled structure. Similarly, replacing the symmetry plane in Figure 2-3 (b) by a magnetic wall (or an open circuit) results in a single resonant circuit having a resonant frequency given by

$$f_e = \frac{1}{2\pi\sqrt{L(C-C_m)}} \quad \text{.....(2-8)}$$

In this case, the coupling effect reduces the capability to store charge so that the resonant frequency is increased. Equations (2-7) and (2-8) can be used to find the electric coupling coefficient k_E as

$$K_E = \frac{f_m^2 - f_e^2}{f_m^2 + f_e^2} = \frac{C_m}{C} \quad \text{.....(2-9)}$$

The above equation coincides with the definition of the ratio of the coupled electric energy to the stored energy of an uncoupled single resonator.

2.3.1.2 Magnetic Coupling

Figure 2-4(a) shows an equivalent lumped-element circuit for magnetic coupling structures, where L and C are the self-inductance and self-capacitance, and L_m represents the mutual inductance.

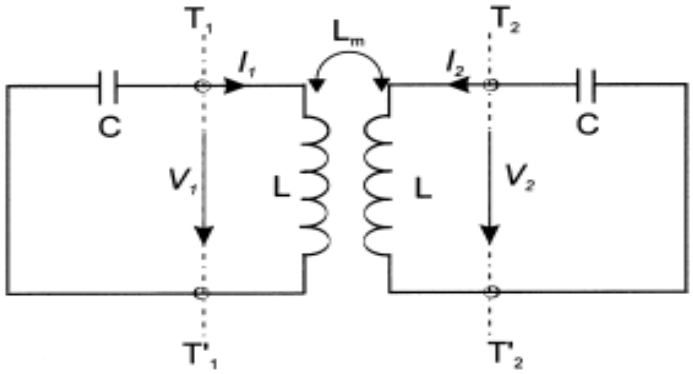

(a)

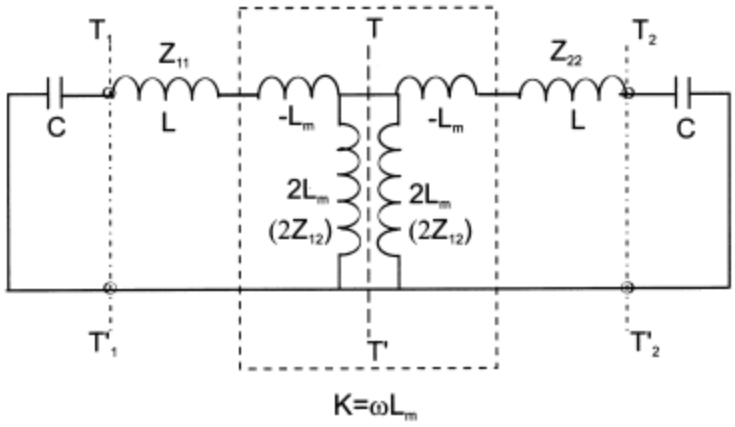

(b)

Figure 2.4 (a) Synchronously tuned coupled resonator circuit with magnetic coupling. (b) An alternative form of the equivalent circuit with an impedance inverter $K = \omega L_m$ to represent the coupling.

In this case, the coupling equations explaining the two-port network at reference planes T_1–T_1' and T_2–T_2' are

$$V_1 = j\omega L I_1 - j\omega L_m I_2 \quad \text{.....(2-10)}$$

$$V_2 = j\omega L I_2 - j\omega L_m I_1 \quad \text{.....(2-11)}$$

The equations in (2-10) and (2-11) also imply that the self-inductance L is the inductance seen in one resonant loop of Figure 2-4(a) when the adjacent loop is open-circuited. Thus, the terms on the R.H.S. of (2-11) are the induced voltages resulting from the increasing current in loops 2 and 1, respectively. It should be noticed that the two loop currents in Figure 2-4(a) flow in the opposite directions, so that the voltage drops due to the mutual inductance have a positive sign. From (2-10) and (2-11) we can find Z parameters as

$$Z_{11} = Z_{22} = j\omega L \quad \text{.....(2-12)}$$

$$Z_{12} = Z_{21} = j\omega L_m \quad \text{.....(2-13)}$$

Figures 2-4 (b) show an alternative form of equivalent circuit which the microwave network parameters are the same as those in Figure 2-4 (a). It can be seen that the magnetic coupling between the two resonant loops is represented by an impedance inverter $K = \omega L_m$. If the

symmetry plane *T–T'* in Figure 2-4 (b) is replaced by an electric wall (or a short circuit), the resonant frequency of resultant single resonant circuit can be written as

$$f_e = \frac{1}{2\pi\sqrt{C(L-L_m)}} \quad \text{.....(2-14)}$$

It can be seen that as the resonant frequency increases due to the coupling effect, the stored flux in the single resonator circuit is decreased when the electric wall is introduced to the symmetric plane. If a magnetic wall (or an open circuit) changes the symmetry plane in Figure 2-4 (b), the resonant frequency of resultant single resonant circuit can be written as

$$f_m = \frac{1}{2\pi\sqrt{C(L+L_m)}} \quad \text{.....(2-15)}$$

In this case, it turns out that the stored flux is increased by the coupling effect, so that the resonant frequency becomes lower. Similarly, (2-14) and (2-15) can be used to calculate the magnetic coupling coefficient K_M as

$$K_M = \frac{f_e^2 - f_m^2}{f_e^2 + f_m^2} = \frac{L_m}{L} \quad \text{.....(2-16)}$$

It should be noticed that the magnetic coupling coefficient described by (2-16) corresponds to the definition of the ratio of the coupled magnetic energy to the stored energy of an uncoupled single resonator.

2.3.2 Mixed Coupling

Figure 2-5(a) represents both the electric and magnetic couplings for coupled-resonator structures. Notice that the *Y* parameters are the admittance parameters of a two-port network from the left side of reference plane T_1–T_1' to the right side of reference plane *T2–T2'*, while the *Z* parameters are the impedance parameters of another two-port network between the reference plane T_1–T_1' and the reference plane T_2–T_2'.

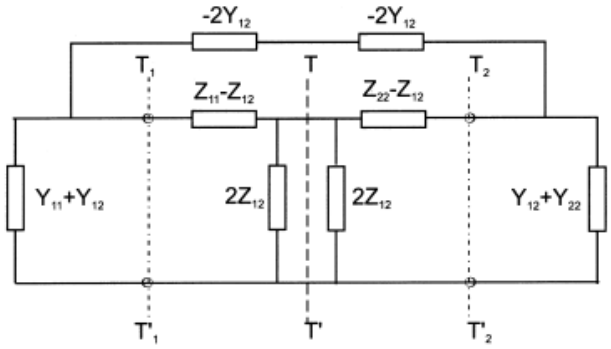

(a)

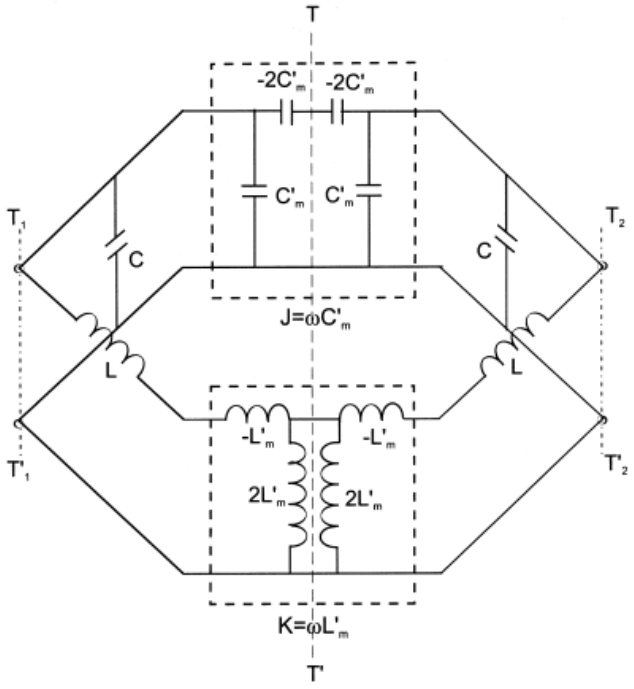

(b)

Figure 2.5 (a) Network representation of mixed coupled resonator circuit (b) An equivalent circuit with an impedance inverter $K = \omega L'_m$ and an admittance inverter $J = \omega C'_m$ to represent the magnetic coupling and electric coupling, respectively

The Y and Z parameters are defined by

$$Z_{11} = Z_{22} = j\omega L \quad \text{.....(2-17)}$$

$$Z_{12} = Z_{21} = j\omega L'_m \quad \text{.....(2-18)}$$

$$Y_{11} = Y_{22} = j\omega C \quad \text{.....(2-19)}$$

$$Y_{12} = Y_{21} = j\omega C'_m \quad \text{.....(2-20)}$$

where C, L, C'_m, and L'_m are the self-capacitance, the self-inductance, the mutual capacitance, and the mutual inductance of an equivalent lumped-element circuit as shown in Figure 2-5(b). One can also identify an impedance inverter $K = \omega L'_m$ and an admittance inverter $J = \omega C'_m$, which represent the magnetic coupling and the electric coupling, respectively.

By inserting an electric wall and a magnetic wall, respectively, into the symmetry plane of the equivalent circuit in Figure 2-5(b) we obtain

$$f_e = \frac{1}{2\pi\sqrt{(C-C_m)(L-L_m)}} \quad \text{.....(2-21)}$$

$$f_m = \frac{1}{2\pi\sqrt{(C+C_m)(L+L_m)}} \quad \text{.....(2-22)}$$

In this case, the resonant frequency shift is caused by both the magnetic and electric couplings. From (2-21) and (2-22), the mixed coupling coefficient k_x can be obtained as

$$K_X = \frac{f_e^2 - f_m^2}{f_e^2 + f_m^2} = \frac{CL'_m + LC'_m}{LC + L'_m C'_m} \quad \text{.....(2-23)}$$

It is reasonable to assume that $L'_m C'_m << LC$, and thus equation (Eqn.2-23) becomes

$$K_X = \frac{L'_m}{L} + \frac{C'_m}{C} = K'_M + K'_E \quad \text{.....(2-24)}$$

which clearly indicates that the magnetic and electric couplings should be taken into consideration in the mixed coupling results from the superposition because the superposition of both the magnetic and electric couplings can result in two opposite effects, either enhancing or canceling each other as mentioned before. If we allow either the mutual inductance or the mutual capacitance in Figure 2-5(b) to change sign, we will find that both couplings tend to cancel each other out.

It should be noticed that for numerical computations, depending on the particular EM simulator used, as well as the coupling structure analyzed, it may sometimes be difficult to implement the electric wall, the magnetic wall, or even both in the simulation. This difficulty can be solved by analyzing or calculating the whole coupling structure instead of the half, and finding the natural resonant frequencies of two resonant peaks, observable from the resonant frequency response. It has been proved that the two natural resonant frequencies obtained in this way are f_e and f_m.

2.4 General Formula for Extracting Coupling Coefficient *k*

The formulas for extracting the magnetic, electric, and mixed coupling coefficients have been derived in terms of the characteristic frequencies of coupled resonators. It is interesting to know that the formulas are all the same. Therefore, we may use the following general expression:

$$K = \pm\frac{1}{2}\left(\frac{f_{02}}{f_{01}} + \frac{f_{01}}{f_{02}}\right)\sqrt{\left(\frac{f_{p2}^2 - f_{p1}^2}{f_{p2}^2 + f_{p1}^2}\right)^2 - \left(\frac{f_{p02}^2 - f_{p01}^2}{f_{p02}^2 + f_{p01}^2}\right)^2} \quad \text{.....(2-25)}$$

where $f_{0i} = \omega_{0i}/2\pi$ and $f_{pi} = \omega_i/2\pi$ for i= 1, 2. The expression of (2-25) is available to extract the coupling coefficient of two coupled resonators, regardless of whether the coupling is electric, magnetic, or mixed. Needless to say, the expression can be used for synchronously tuned coupled resonators as well, and in that case, it simplifies to

$$K = \pm\frac{f_{p2}^2 - f_{p1}^2}{f_{p2}^2 + f_{p1}^2} \quad \text{.....(2-26)}$$

where f_{p1} or f_{p2} corresponds to either f_e or f_m. The sign of coupling may only be a matter for cross-coupled resonator filters. It should be kept in mind that the determination of the sign of the coupling coefficient is much dependent on the physical coupling structure of coupled resonators. Nevertheless, for filter design, the meaning of negative or positive coupling is rather relative. This means that if we refer to one particular coupling as the positive coupling, and then the negative coupling would imply that its phase response is opposite to that of the positive coupling. The phase response of a coupling may be found from the S parameters of its associated coupling structure. Alternatively, the derivations in Sub Chapter 2.2 have suggested another simple way to find whether the two coupling structures have the same signs or not. This can be done by introducing either the electric or magnetic wall to find the f_e or f_m of both the coupling structures. If the frequency shifts because of f_e or f_m with respect to their individual uncoupled resonant frequencies are in the same direction, the resultant coupling coefficients will have the same signs, if not then the opposite signs. For instance, the electric and magnetic couplings discussed in Sub Chapter 2.2 are said to have the opposite signs of their coupling coefficients.

2.5 General Formula for Extracting Quality Factor Q_e

The tapped line and the coupled line structures are two typical input/output (I/O) feed structures for coupled microstrip resonator filters. They are shown in Figure 2-6 with a microstrip open-loop resonator, though other types of resonators may be used. For the tapped-line feed,

usually a 50 Ohm feed line is directly tapped onto the I/O resonator, and the coupling or the external quality factor is controlled by the tapping position *t*, as indicated in Figure 2-6(a). For example, the smaller the *t*, the closer is the tapped line to a virtual grounding of the resonator, which results in a weaker coupling or a larger external quality factor.

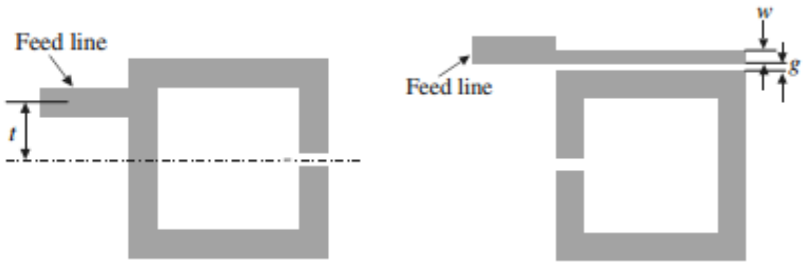

Figure 2.6 Typical I/O coupling structures for coupled resonator filters. (a) Tapped-line coupling. (b) Coupled-line coupling.

The coupling of the coupled line structure in *Figure 2.6* (b) can be determined from the coupling gap *g* and the line width *w*. Normally, a smaller gap and a narrower line result in a stronger I/O coupling or a smaller external quality factor of the resonator.

The external quality factor of a single resonator can be derived in terms of the normalized input admittance (y_{in}) and the group delay (τ_Γ) with respect to the reflection coefficient at the resonant angular frequency ω_0 That is

$$Q_e = \frac{\omega_0 \tau_\Gamma(\omega_0)}{4}[1 - y_{in}^2(\omega_0)] \qquad \text{.....(2-27)}$$

where y_{in} and τ_Γ can be obtained from the reflection coefficient and the derivative of its phase with respect to angular frequency, respectively. As a result, Figure 2-6 shows the value of Q_e as a function of the tapped position (P_t) of the input/output port. Note that the results shown in Figures 2-4(a) and 2.4(b) are based on full-wave electromagnetic (EM) simulation using Ansys-Ansoft HFSS.

2.6 Multilayer BPFs

Recently, there has been increasing interest in multilayer BPFs to meet the challenges of high performance, miniaturized size, and cost requirements. Multilayer BPF technology also provides another dimension in the integration of other microwave components, circuits, and subsystems. Multilayer BPFs can be divided into two main categories. The first category contains various coupled-line resonators that are located on different layers without any ground planes inserted between the adjacent layers. This type of multilayer structure is illustrated in Figure 2-7(a). The second category of the multilayer BPFs utilize aperture couplings on common ground between adjacent layers. The general multilayer structure of this type is depicted in Figure 2-7(b). The BPFs in the first category are more suitable for wide-band applications because the couplings between resonators are stronger. On the other hand, the BPFs in the second category are more suitable for narrow-band applications. Needless to say, the combination of these two types of multilayer structures is possible.

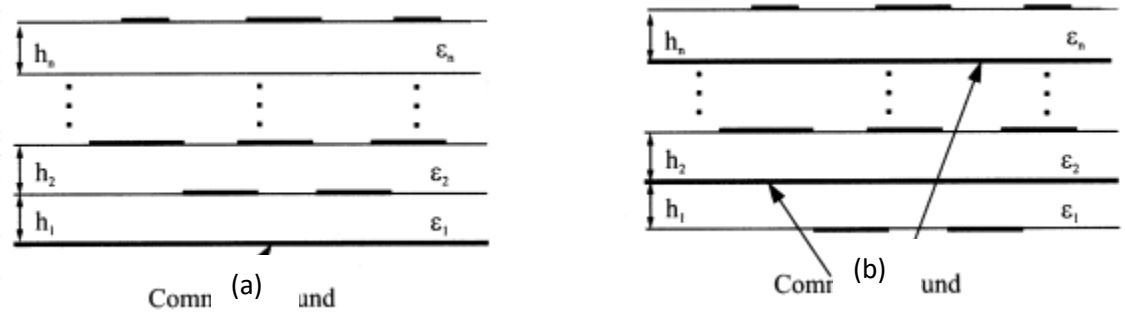

Figure 2.7 Typical multilayer structures. (a) Without any ground plane between the adjacent layers. (b) With ground plane between the adjacent layers